Spatio-Temporal Density Mapping for Spatially Extended Dynamic Phenomena

- a Novel Approach to Incorporate Movements in Density Maps

Stefan Peters
Department of Geoinformation
Universiti Teknologi Malaysia
Johor Bahru, Malaysia
e-mail: stefan.peters@directbox.com

Liqiu Meng
Department of Cartography
Technische Universität München
München, Germany
e-mail: liqiu.meng@bv.tum.de

Abstract - **The visualization of density information and its changes is a crucial support for the spatio-temporal analysis of dynamic phenomena. Existing density map approaches mainly apply to datasets with two different moments of time and thus do not provide adequate solutions for density mapping of dynamic points belonging to the same moving phenomena. The proposed approach termed as Spatio-Temporal Density Mapping intends to fill this research gap by incorporating and visualizing the temporal change of a point cluster in a 2D density map. At first either straight or curved movement trajectories based on centroids of spatio-temporal point clusters are detected. The traditional Kernel density contour surface is then divided into temporal segments, which are visually distinguished from one another by means of a rainbow color scheme. Furthermore, several ideas for the investigation of the usability of our approach are addressed.**

Keywords - spatio temporal density map; rainbow color scheme; visual analytics; dynamic phenomena.

I. INTRODUCTION

As stated in a previous work by Peters and Meng [1], visualization helps to investigate and understand complex relationships in a spatial context. Maps account as one of the most powerful visualization forms. They represent geographic information in abstract ways that support the identification of spatial patterns and the interpretation of spatial phenomena. Furthermore, the visual presentation and analysis of dynamic data and dynamic phenomena is currently a hot research topic [2].

Hence, in today's society, the need for data abstraction along with the growing amount of available digital geodata is rapidly increasing. One reasonable way of abstracting data is provided by density maps [3]. Density maps can be applied for point data in various fields, for instance, in physical or human geography, geology, medicine, economy or biology [4, 5]. How to present the density for dynamic data/phenomena is, however, not yet adequately addressed.

In this paper, we introduce a novel density mapping approach for spatially and temporally changing data. The approach is based on [1], whereby in this work a different test dataset was used, two different types of movement trajectory concepts are introduced, a verification of the used rainbow color scheme is presented, investigations about wrongly assigned points are considered and a more detailed comparison between STDmap and its alternative in form of Kernel Density Estimation (KDE) maps for each temporal interval is provided.

In the next section, the state of the art related to density maps, in particular, an overview of approaches considering the dynamics of movement data in the density visualization is given. In the section afterwards, our own approach is described in detail, followed by implementation processes, discussions of the results and a conclusion.

II. DENSITY MAPS - STATE OF THE ART

One of the most straight forward ways to visualize point density is a scatter plot or a dot map. Graphic variables for point symbols, such as size, shape, color and transparency, can be applied in relation with the attribute value. In order to discern the density distribution, these graphic variables can be iteratively adapted to the given map scale, but still the occlusion of neighboring points cannot be always desirably avoided. The density value of each point can be obtained by counting all points within a buffer around the point or within a grid cell the point is located in.

In the following, the density estimation and map principles are shortly presented and the state of the art of density maps with static or dynamic data is given.

A. KDE

KDE [6] is a classic method widely used to determine densities of individual points that represent a continuous surface. The KDE approach is described in detail in [6-8]. The standard KDE, a normal distribution function, uses a Gaussian kernel:

$$\widehat{f}_h(x) = \frac{1}{n \cdot h} \sum_{i=1}^{n} K(u) \tag{1}$$

whereby $u = \dfrac{X - X_i}{h}$ and $K_G(u) = \dfrac{1}{\sqrt{2\pi}} \cdot \exp\left(-\dfrac{1}{2}u^2\right)$

with:

$\widehat{f}_h(x)$	=	general Kernel density function
K	=	Kernel function
K_G	=	standard Gaussian function
h	=	smoothing parameter (bandwidth)
n	=	number of points
X	=	point (x,y) for which the density will be estimated
$X_1, X_2, \ldots, X_N$	=	sample points, placed within the kernel radius h

Beside a Gaussian kernel, also other kernel types can be applied, such as Triangular, Biweight, Epanechnikov or Uniform kernel [7]. A certain bandwidth (search radius) is defined for the kernels, located around each point. For each cell of an underlying grid (defined by a certain resolution) a density value is calculated as shown in equation (1) and hence a smooth surface is provided [9]. The kernel bandwidth value strongly effects the resulting density surface [10]. A formula for an optimal bandwidth is offered by Silverman [7] as shown in equation (2).

$$bw\_optimal = 1.06 * \min\left(\sqrt{\mathrm{var}(P)}, \frac{\mathrm{IQR}(P)}{1.34}\right) * n^{-\frac{1}{5}} \quad (2)$$

with: $bw\_optimal$ = optimal bandwidth
P = point dataset (coordinates)
IQR(P) = interquartile range
var(P) = variance of P
n = number of points

In order to detect clusters, KDE has been applied in in various applications, such as crime analysis and population analysis. Kwan [11] used KDE and 3D visualization to investigate spatio-temporal human activity patterns. The author applied the density estimation as a method of geovisualization to find patterns in human activities related to other social attributes. The classic KDE was investigated in [12-14], and thereby defined as a visual clustering method. In these works, KDE maps were created in order to visually provide a better overview and insight into the given data.

B. Contour lines and intervals

A common technique to map point densities calculated using KDE are isopleth maps with filled contour intervals. The term "isopleth map" refers to one of two types of isoline maps (also called isarithmic or contour maps). In the first type of isoline maps each contour line indicates a constant rate or ratio derived from the values of a buffer zone or kernel area. In this sense, the continuous density surface is derived from an originally discrete surface. In the other type of isoline maps (commonly referred to "isometric map"), contour lines (isometers) are drawn through points with directly measurable equal value or intensity such as terrain height or temperature [15]. It is assumed that the data collected for enumeration units are part of a smooth, inherently continuous phenomenon [16]. In our context, we only use contour lines to delimit the intervals (the areas between contour lines).

Furthermore, Langford and Unwin [17] provided a good overview of density surfaces used in Geographic Information Systems (GIS) as choropleth population density maps, population density on grids, population density surfaces, and pseudo-3D population density surfaces. In several works as [4, 5], the KDE concept is adapted for the 3D space density mapping of static 3D data.

C. Dynamic data and density information

In the following sections, an overview is given about existing works related to density maps of dynamic points.

1) Sequence of KDE maps for dynamic points

A straightforward way of visualizing the density of dynamic points would be a sequence of density surfaces (one per time interval). The change of the density in time could be better discernable by means of an animation of these density maps. We could also arrange the local density contours of each time interval on the same map. Transparency and a unique color scheme for each time interval could be applied in order to distinguish different density contours. However, the tinted intervals may spatially overlap and make the map reading a difficult endeavor.

2) Dual KDE

Jansenberger and Staufer-Steinocher [18] analyzed two different point datasets recorded within the same area, but at two different moments of time. The authors suggest a Dual-KDE approach, which results in a map illustrating the spatio-temporal density difference of the two datasets. The absolute difference is used, that is, the absolute density of the second point dataset subtracted from that of the first one.

3) DKDE

The approach called Directed Kernel Density Estimation (DKDE) that takes the dynamics of moving points inside density maps into account was suggested in previous works [19-24]. The DKDE is applicable for discrete moving points and it considers two moments of time. Instead of an upright kernel as in the KDE method, a tilted kernel is used, as illustrated in Figure 1.

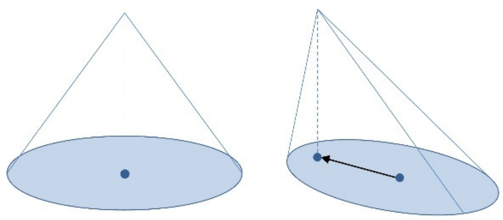

Figure 1. Linear kernel (left) and Directed linear kernel taking point speed and movement direction into account (right), source: [24].

The tilt depends on the movement direction vector of the respective point. The resulting DKDE-map shows the so-called "ripples", which can be interpreted as an indicator for the movement direction and density change of points that are located closely to each other with very similar movement speeds and directions. These ripples are visible among overlapped contour lines. The tinted contour intervals do not contain the information about movement or density change.

Peters and Krisp [24], for instance, used 2D airplane positions in the area of Germany at two moments of time with a time lag of five minutes. The resulting DKDE-map is shown in Figure 2.

2015, © Copyright by authors, Published under agreement with IARIA - www.iaria.org

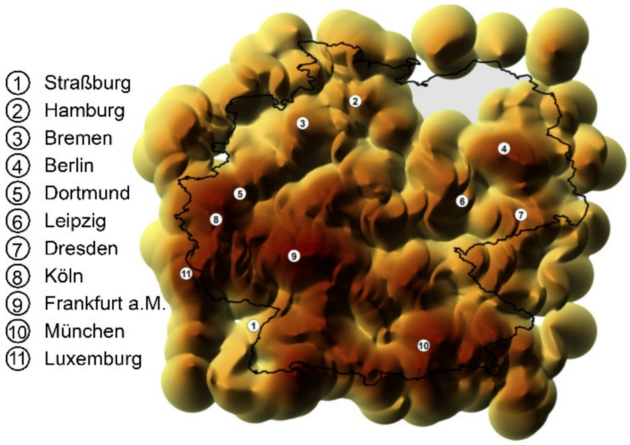

Figure 2. DKDE-map based on airplane positions at two moments of time, source: [24].

4) 3D density map using space time cube (STC)

Nakaya and Yano [25] suggest a method using a STC to visually explore the spatio-temporal density distribution of crime data in an interactive 3D GIS. Thereby the author adapted the KDE by using space-time variants and scan statistics. In order to investigate the dynamics and density change, an interactive use within a 3D environment is essential.

5) KDE for trajectories

In a comprehensive review, Andrienko and Andrienko [2] discussed existing visual analysis methods, tools and concepts for moving objects. A section is dedicated to continuous density surfaces (fields) derived from trajectories or from point-related attributes. Density maps of moving objects were created on the basis of aggregated points of trajectories. A trajectory is understood as a function of time or a path left by a moving object in space. Moving objects can be confined within a network (such as cars along streets of a traffic network) or float freely over a region (boats) or in space (airplanes). Spatio-temporal density maps of trajectories were investigated in [26-29]. In these approaches, the KDE method is adapted to trajectories as a function of changing velocity and direction. Willems et al. [30], for example, built his kernels assuming constant speeds. Furthermore, McArdle et al. [31] investigated computer mouse trajectories. Thereby density maps are generated based on movement activity. For each scale, the density map is recalibrated in order to highlight the most important areas, in terms of mouse movement activity. Other approaches assume constant acceleration. The resulting density maps can reveal simultaneously large-scope patterns and fine features of the trajectories. This mapping idea was extended to the 3D space in [27], where the trajectory densities are visualized inside a STC.

Another possibility of displaying density information of trajectories is to use derived discrete grid cells, whereby each cell color refers to the amount of trajectories passing through the cell [32, 33].

D. Research questions

In the existing 2D density maps based on KDE, the time is either frozen on a certain moment or confined within a certain time interval. Consequently, the resulting contour lines do not carry information of temporal changes. Although various approaches for density visualization of trajectories have been investigated, an appropriate method for 2D density maps of moving point clouds is still missing. Whether the dynamics of spatially extended phenomena (SEPs) - represented by points – can be adequately expressed in a single contour map remains an open question. To tackle this question, we develop an approach termed as Spatio-Temporal Density Mapping or STDmapping.

III. TEST DATASET

We used lightning points recorded by LINET, a lightning detection network [34], as the test dataset. It contains altogether 8184 detected lightning in the region between Munich, Germany and Prague, Czech Republic (47°N–50°N Latitude and 11°E–15°E Longitude) on April 26th 2013 between 2pm and 7pm. Each point is encoded with its geographic coordinates (longitude, latitude) as well as the exact lightning occurrence time. The recorded height information is not considered within our approach.

Figure 3 illustrates the lightning points in form of blue dots projected onto a plane surface. The background base map contains topographic data of the area out of Open Street Map dataset. The use of such static plot of lightning data is limited for the investigation of the dynamics in lightning data. To enhance clarity of the approach, only points of the three largest lightning tracks are considered in the STD density mapping approach.

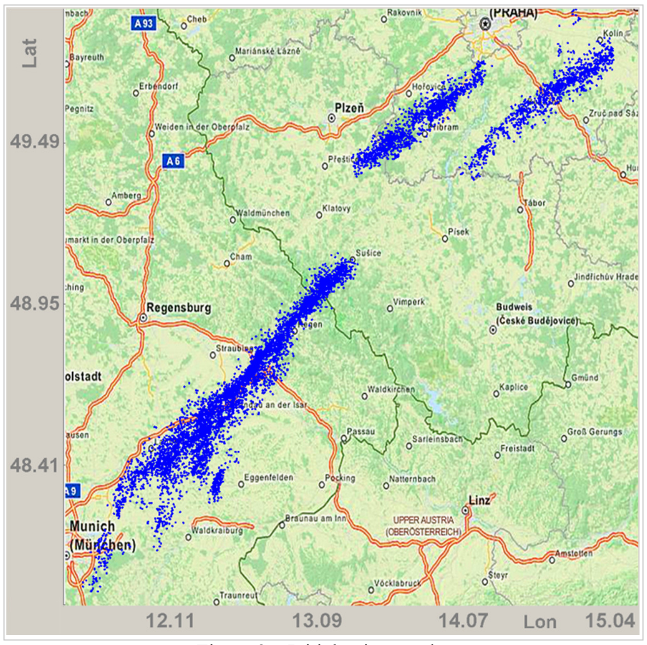

Figure 3. Initial point test dataset.

2015, © Copyright by authors, Published under agreement with IARIA - www.iaria.org

Visual analysis methods for these lightning points, which represent the moving phenomena of a thunderstorm, were published in [35-37].

IV. METHODOLOGY

First of all, density contour maps can be derived from point datasets using KDE while an optimal kernel bandwidth can be calculated according to Silverman's formula [7]. In our work we deal with a lightning point dataset representing a dynamic phenomenon. Thus, instead of creating a single density contour map of the entire point dataset, we applied KDE in each case to all points belonging to the same lightning track. Thereby, lightning points are clustered, afterwards allocated and aggregated to trajectories. In doing so, a temporal clustering is applied to the initial point dataset using a time interval of one hour. Subsequently, all points within each temporal interval are spatially clustered using a buffer threshold of six kilometers. In the resulting spatio-temporal clusters, the spatially overlapping parts within two time sequences are detected and afterwards allocated and aggregated to lightning trajectories. Further details of the temporal and spatial clustering of lightning data including explanations for thresholds can be found in [35, 36]. The results of the density contour maps derived for the test dataset are shown in Figure 4. The importance of grouping dynamic points into tracks is discussed in the next section.

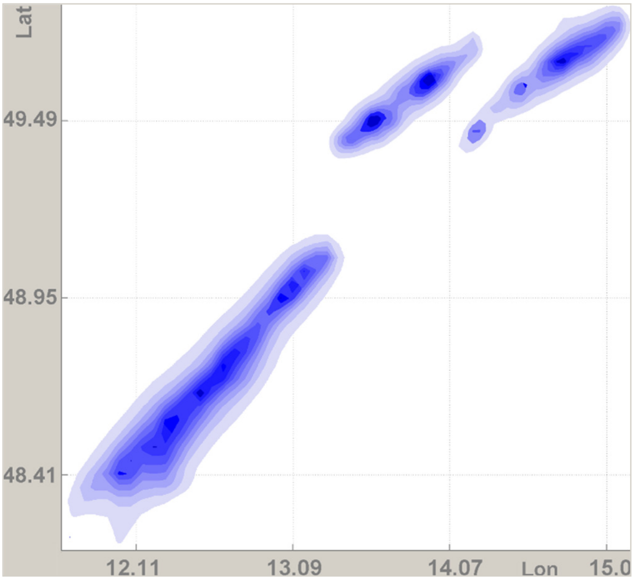

Figure 4. KDE map applied to test point dataset.

The resulting density contour layers in blue tones do not bear any temporal information. Nevertheless, the aforementioned temporal point clustering method provides time information for each lightning point. Figure 5 illustrates our initial point dataset, whereby lightning points were segmented and colored according to the different time intervals, thus reveal the dynamic changes. In doing so, we used a time interval of 1 hour starting at 2pm for the temporal clustering. The overlapping convex hulls surrounding all spatially clustered points of the same temporal interval are allocated to altogether three different trajectories.

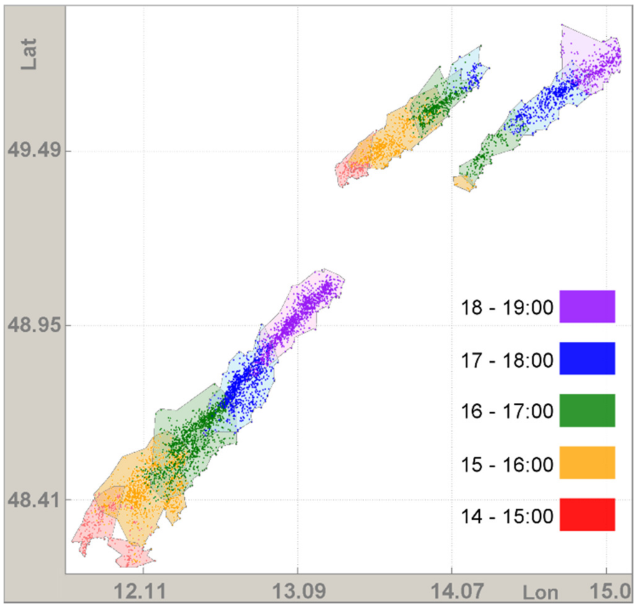

Figure 5. Temporally clustered point data.

Three main moving lightning clusters are perceivable within the test area. Their geographic and temporal locations are apart from each other with one formed at lower left part and one upper left, both starting around 2pm and the third one upper right occurring around 4pm. All clusters are moving north-eastwards. The upper left cluster disappears around 5pm, whereas the lower left and the upper right last until 7pm.

As mentioned before, traditional density mapping does not contain temporal information. Clustering and allocating dynamic point data (in our case lightning points) towards trajectories provides information about data movement (speed, direction, etc.).

In the following, we introduce a method, which includes movement information, i.e., dynamics in KDE mapping. In other words, we suggest a solution to incorporate temporal information of moving points (as illustrated in Figure 5) inside the density contour intervals (as shown in Figure 4).

A. *STDmapping workflow*

An overview of our suggested method is illustrated through an overall workflow in Figure 6.

First of all a density contour map using KDE is created. Additionally, the given point dataset is temporally and spatially clustered. In the next step, the overlapping clusters (in case they are temporally successive) are detected and after that allocated and aggregated to independent tracks. Cluster centroids are embedded in the trajectories. A detailed description about these steps can be found in [35].

2015, © Copyright by authors, Published under agreement with IARIA - www.iaria.org

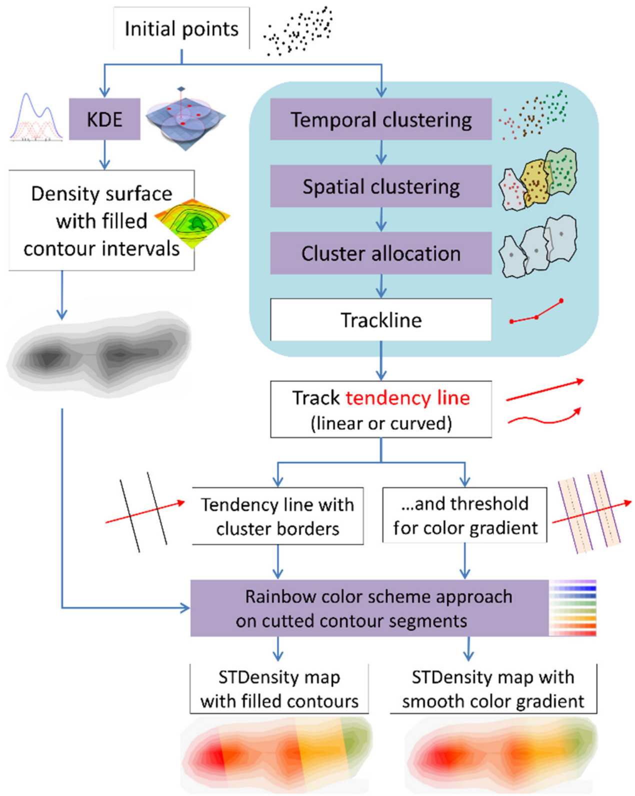

Figure 6. The workflow of STDmapping of lightning data.

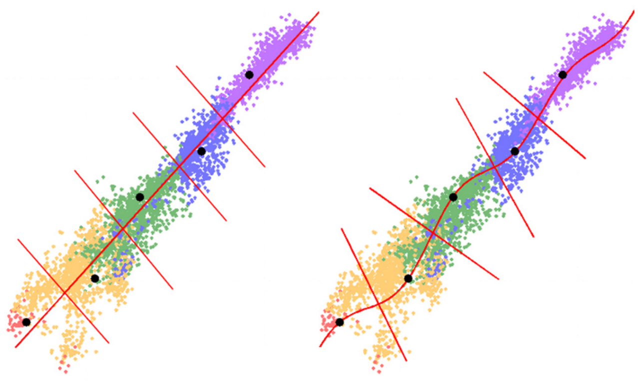

Figure 7. Temporally clustered points and cluster centroids in black with straight tendency line and perpendicular temporal borders (left) and with curved tendency line and perpendicular temporal borders (right).

A linear approximation of each track results in a straight tendency line, which represents the average moving direction of the point cluster. The linear approximation can be based either only on the cluster centroids or on the entire point datasets of a track.

If the projected trajectory is curved rather than straight, the tendency line can be approximated by a polyline connecting the cluster centroids. In our case, a cubic spline interpolation function is used to fit a curve through the cluster centroids [38].

Consequently, we have on the one hand the density surfaces represented by layered tints between neighboring contour lines and on the other hand the tendency line with either abrupt or smooth transition at borders of temporal clusters. This temporal border is a line perpendicular to the tendency line passing through the average locations of all points within a certain period (in our case 10 minutes) before and after a temporal border (e.g., full hour). If the phenomenon is moving, all points between two temporal borders (e.g., between “2pm line” and the “3pm line”) are grouped into the same temporal interval (period: “2pm - 3pm”).

The next question is how we can incorporate the dynamics inside the density map. The idea is to divide the tendency line into temporal parts, which will in turn guide the segmentation of the density surface.

Figure 7 illustrates two different ways of tendency line determination. In the left part, all points of an exemplary lightning track are colored according to the temporal cluster they respectively belong to. The cluster centroids are presented as black dots. A straight tendency line representing the general movement direction of the lightning cluster is based on the coordinates of all cluster centroids. The temporal borders in red are detected and vertically aligned to the straight tendency line. The locations for temporal borders can be defined by the half distance between two temporally successive cluster centroids, or, by the centroid of the overlapping area of two sequential temporal point sets.

In the right part of Figure 7, the tendency line is represented by a curve determined through cubic spline interpolation of all cluster centroids. The temporal borders in red are defined again as perpendicular lines of the curved tendency line. Thus, temporal border lines are not arranged parallel to each other as in the case for the straight tendency line. However, for very small temporal clusters (clusters of low velocity or very small temporal thresholds) temporal border lines are much closer to each other, and thus – due to the curved tendency line route – they are almost parallel to each other.

Nevertheless, it could be also possible that two sequential temporal borderlines intersect each other (in particular if the tendency line is strongly curved). In this case, the respective intersecting temporal borderlines need to be partly merged as shown in Figure 8. Thereby, different temporal segments are illustrated in different colors (beige, green, blue) and temporal borders in red. We suggest combining the two intersecting temporal border lines from the intersection point onwards towards the outer cluster extension in a way that each of both temporal border lines forms the same angle with the continuing merged border line part.

2015, © Copyright by authors, Published under agreement with IARIA - www.iaria.org

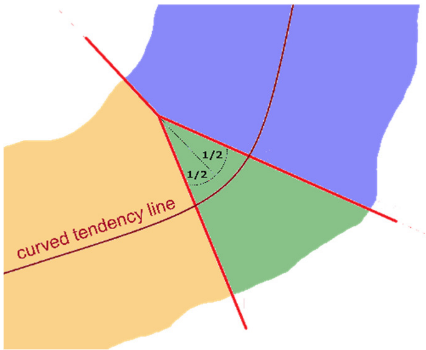

Figure 8. Suggested solution for intersecting temporal border lines (red).

In the next step, density contours are separated through temporal borderlines into temporal surface segments as illustrated in Figure 9.

As described before, temporal borders can be either parallel if they are based on a straight tendency line (see Figure 9 left) or temporal borders are perpendicular to the curved tendency line and thus non-parallel (see Figure 9 right).

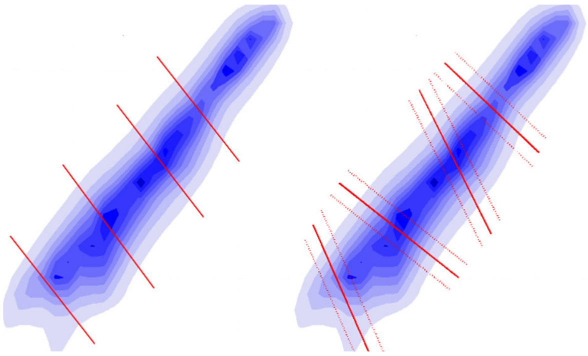

Figure 9. Density contours with temporal borders based on a linear tendency line (left) and with temporal borders and thresholds for smooth color gradients based on a curved tendency line (right).

Furthermore, thresholds for temporal borderlines can be applied for smooth color transitions. Different temporal surface segments carry different color hues. Within the same surface segment, the color hue remains the same but its intensity varies with the change of density.

In our approach, we adopted the “rainbow color scheme”, which is essentially the visible and continuous electromagnetic spectrum. Its main color hues transit from red, orange, yellow, green, blue to violet. The spectrum can be divided into an arbitrary number of intervals. Users may easily anticipate and comprehend the color transitions. In our approach, we assign each time interval to a certain color hue – the medium color of the rainbow subinterval.

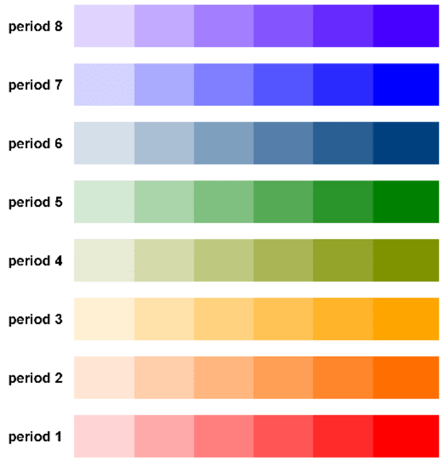

Figure 10. Rainbow color scheme.

Figure 10 exemplary illustrates eight different rainbow color hues with each being displayed in up to six different color intensities from light to dark. For instance, the red color scheme refers to time period 1 and contains six different red tones, which are related to six different density values/ value intervals. We split the entire time of our dynamic dataset into equal time intervals. The interval size can be determined based on the user’s interest.

Hue represents time (e.g., discretized at 1 hour intervals) and color intensity corresponds to the density of observations (low intensity refers to low density and high intensity to high density). A continuous color scheme should not include more than three hues; otherwise the visual perception may suffer. An exception is the rainbow scheme. Most people know the differences in short and long wavelengths of visible light and are therefore familiar with the rainbow color gradation.

We decided to use the rainbow color scheme in order to fulfill the following two criteria:

‘*Clear differentiation*’: colors of adjacent segments should be clearly distinguishable from each other. In particular, the brightness spectrum from low to high intensity should be distinct for each color hue from those of the others.

‘*Continuity*’: The color hues including their different intensities should represent the movement, thus, consists of a continuous color gradation. From the first hue allocated to the first temporal interval to the last one, the map user should be able to visually detect this continuity through a continuous color scheme. This color scheme has to be commonly known/familiar and intuitively understandable.

In literature, rainbow color maps are commonly used, but often are considered as harmful for continuous data [39]. The arguments against rainbow schemes include the inappropriateness for colorblind people, the appearing of divisions between hues, which lead to visual “edges” in the map, the meaningless spectral order of the hues and difficulties to recognize details. In particular to differentiate qualitative and quantitative attributes through polygon hue, the use of the rainbow scheme is often criticized. Figure 11

2015, © Copyright by authors, Published under agreement with IARIA - www.iaria.org

illustrates five different color scheme approaches for the STDmap using the rainbow color scheme (a) and four alternatives involving a color gradient from blue to purple (b) as well as three color scheme from Colorbrewer.org [40]: diverging (c), sequential multiple hues (d) and sequential single hue (e).

To visualize continuous data, often bipolar color illustration is used. On the other hand, also the rainbow color scheme is frequently used, for example to visualize the earth gravitational field (geoid anomalies) or illustrate weather-related intensities, such as storm severity [41]. Although the rainbow color scheme with its color gradation is commonly known, the continuity information based on color gradation might be easier to identify in the options provided in Figure 11-b,c,d,e. However, in Figure 11-c,d,e individual contour segments are difficult to identify due to the use of/color transition to white or yellow. Although the movement of the spatially extended object (SEO) in time is clearly visible in Figure 11-b, individual neighboring temporal segments could be confusing – which is not the case in Figure 11-a. To fulfill/combine the two contradictory criteria of the continuity and the clear differentiation, we have to make a compromise. The rainbow scheme might be more appropriate for some cases while a continuous color scheme involving 2-3 hues might suit better for other applications. For our STDmapping approach, we preferred to use the rainbow scheme. However, a user test is needed to verify the proper use of rainbow color scheme for our STDmap.

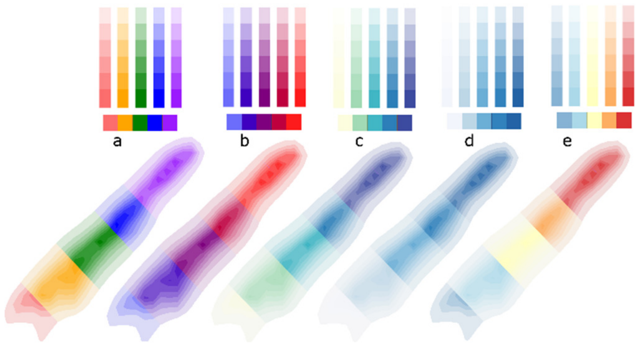

Figure 11. Different color scheme approaches.

With regard to the division of density surface by means of the temporal tendency lines (following either a straight or a curved route), we introduce the perpendicular lines to each tendency line as the temporal borders between the two neighboring time intervals of the underlying KDE map. The color transition between two temporal segments can be either abrupt or smooth. In case of smooth temporal borders, a defined threshold for the smooth color transition is set. The threshold refers to a certain time before and after the abrupt temporal borders. That leads to two parallel border lines – one to the left, the other to the right of the abrupt border line. The distance (time) between each smooth border line and the respective abrupt border line can be constant and variable.

Thus, our STDmapping approach provides a solution for the visual incorporation of temporal information within density surfaces of layered tints.

V. Results and Discussion

For applying density visualization to our test dataset, containing lightning points during April 26th 2013, we used both our proposed STDmapping approach and the commonly used KDE method. Applying the latter traditionally for each spatio-temporal cluster, a segment of density map with layered tints was produced as illustrated in Figure 12, which however is not satisfying due to parts of overlays and occlusion. It leads to a loss of certain local and of the overall density information.

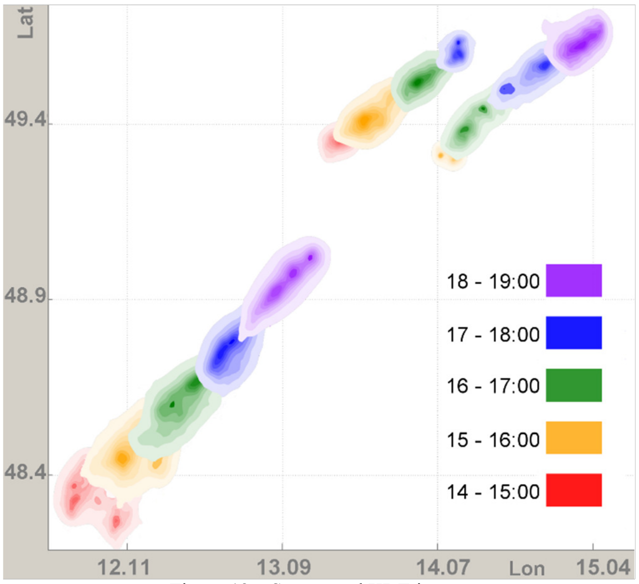

Figure 12. Segmented KDE in one map.

Applying transparency does not solve this drawback adequately. Due to the fact, that the density contour intervals of each temporal interval have the same hue but differ in color intensities, a transparency changes the intervals with low intensities to almost invisible – even if a contour border with a slightly more intense color is added. Hidden parts of overlapped contour intervals will still not be sufficiently recognizable.

Thus, using KDE maps for each spatio-temporal cluster provides only direct depiction of time for non-overlapping contour surfaces. Furthermore, visual exploration of density information in the overlapping parts is only possible for the surface on top; in case transparency is applied it is very difficult. Another disadvantage occurs when one is interested in density information including points detected shortly before and after the temporal interval border.

By applying the new STDmapping approach to our test dataset and following the workflow in Figure 6, we created eight different output maps (Figure 13 - Figure 20). The temporal borders were based on either straight (*A*) or curved lightning cluster moving tendency lines (*B*). Furthermore, we used two different temporal thresholds: one hour, respectively 30 minutes. Moreover, we applied the abrupt and the smooth concept for color gradients between temporal segments.

A. STDmaps based on straight tendency lines

Four figures illustrate results for spatio-temporal density maps (STDmaps) based on straight tendency lines with the interval of one hour in Figure 13 and Figure 14 and 30 minutes in Figure 15 and Figure 16. The color gradients between temporal borders are abrupt in Figure 13 and Figure 15 and smooth in Figure 14 and Figure 16.

Using straight tendency lines, the temporal borders appear parallel to each other, in particular with abrupt color gradients. Larger distances between sequential temporal borders refer to a faster movement phase of the dynamic phenomenon, whereas the closer successive temporal borders indicate a slower movement of the lightning clusters.

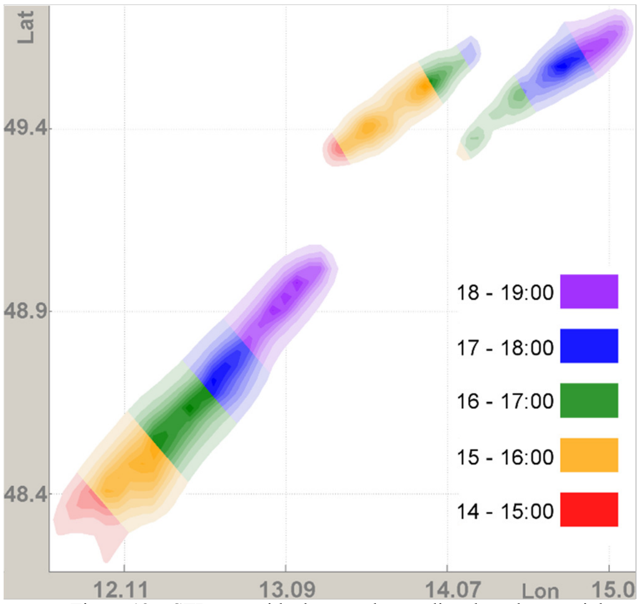

Figure 13. STDmap with abrupt color gradient based on straight tendency lines and the temporal interval of one hour.

When fewer temporal segments are used (e.g., five segments in Figure 13), the map reader may fast and easily extract the distinctive temporal information. When a larger number of temporal segments are used (e.g., in Figure 15), the map reader has to distinguish between more different colors referring to temporal information. This explorative interpretation becomes more effortful. On the other hand, more temporal segments reveal more details and may thus enable a more comprehensive insight in the dynamics of the data (e.g., temporal change of local point density).

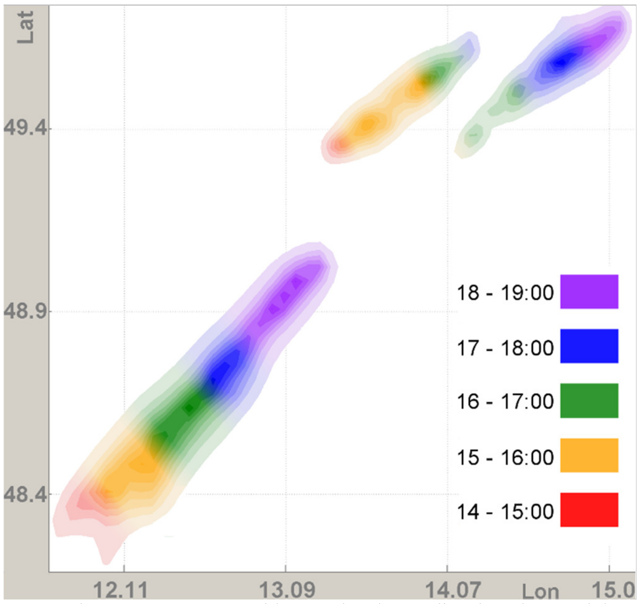

Figure 14. STDmap with smooth color gradient based on straight tendency lines and the temporal interval of one hour.

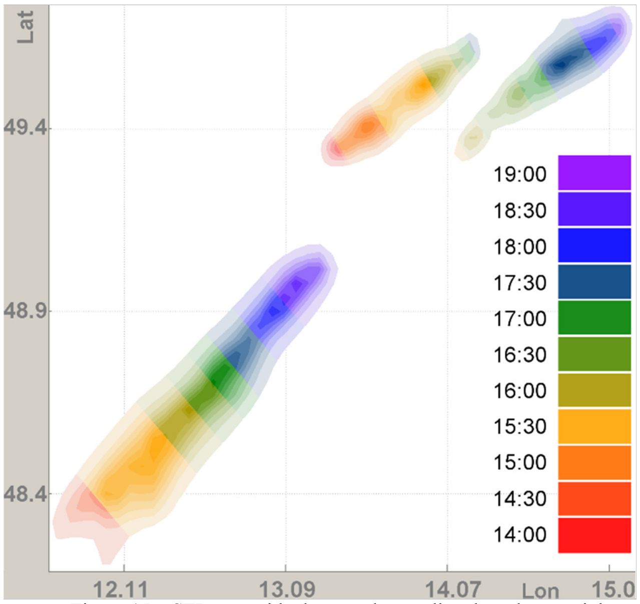

Figure 15. STDmap with abrupt color gradient based on straight tendency lines and the temporal interval of 30 minutes.

2015, © Copyright by authors, Published under agreement with IARIA - www.iaria.org

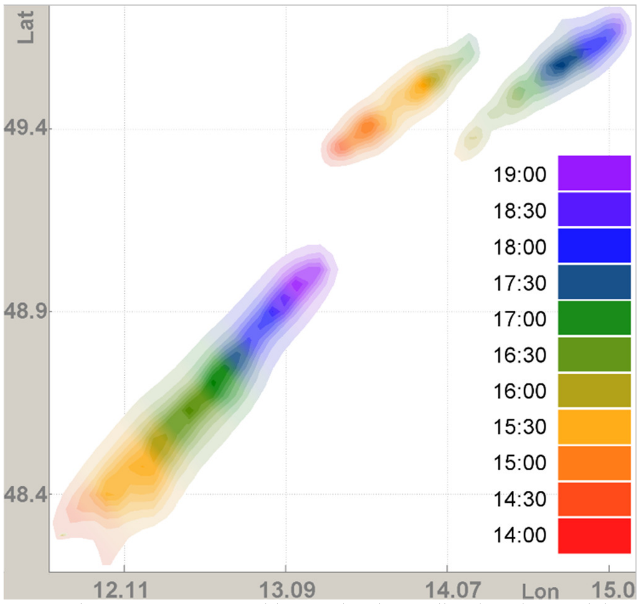

Figure 16. STDmap with smooth color gradient based on straight tendency lines and the temporal interval of 30 minutes.

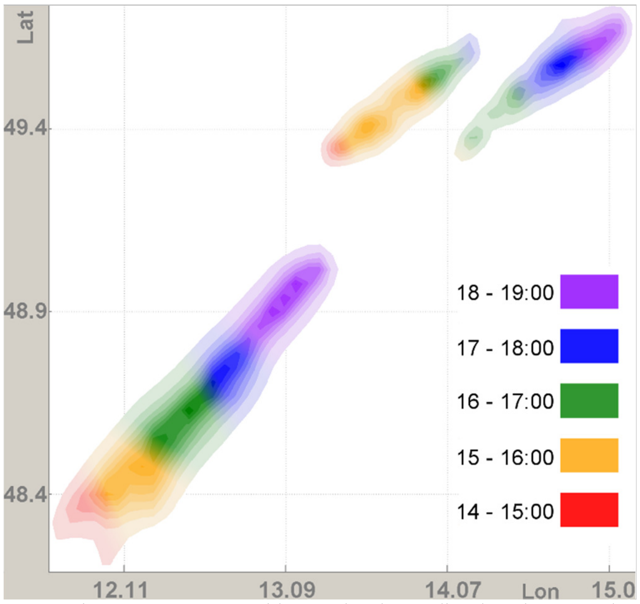

Figure 18. STDmap with smooth color gradient based on curved tendency line the temporal interval of one hour.

B. *STDmap based on curved tendency lines*

Four further figures illustrate the results for STDmaps based on curved tendency lines. The interval of one hour was used in Figure 17 and Figure 18 and 30 minutes for Figure 19 and Figure 20. The color gradients between temporal borders are abrupt in Figure 17 and Figure 19 and smooth in Figure 18 and Figure 20.

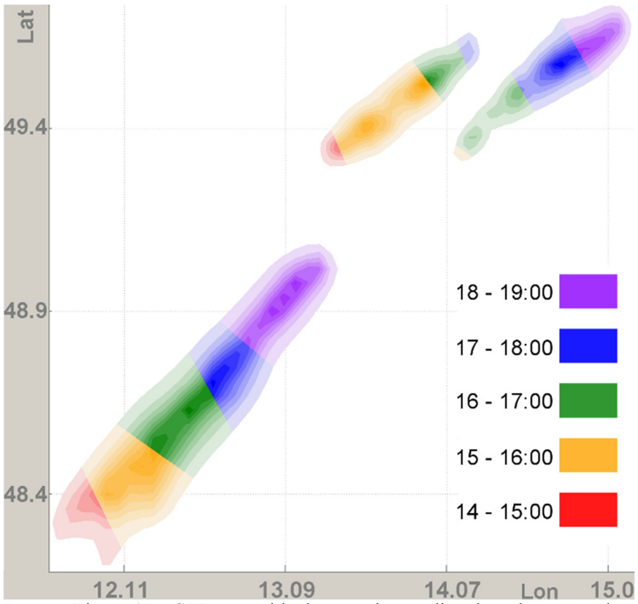

Figure 17. STDmap with abrupt color gradient based on curved tendency line and the temporal interval of one hour.

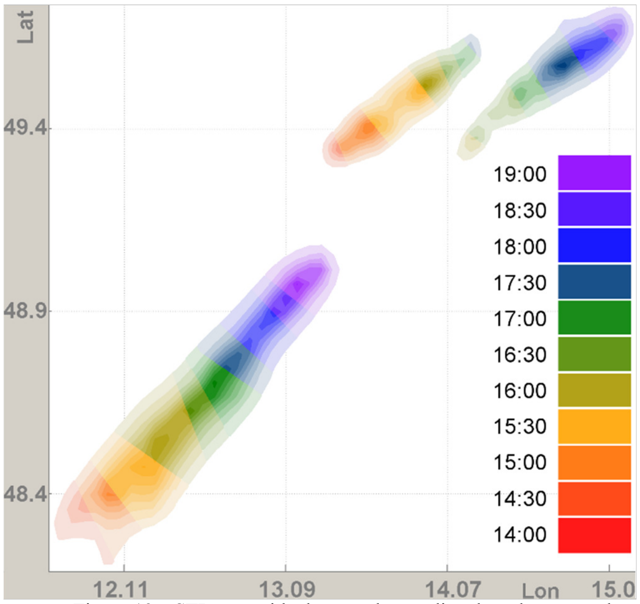

Figure 19. STDmap with abrupt color gradient based on curved tendency line and the temporal interval of 30 minutes.

A comparison of the results from the straight tendency line with those from the curved tendency line (e.g., Figure 14 with Figure 18 using five temporal segments or Figure 16 with Figure 20 using 11 temporal intervals) clearly shows the visual similarity of STDmaps, particularly in case of a rather large threshold for temporal borders.

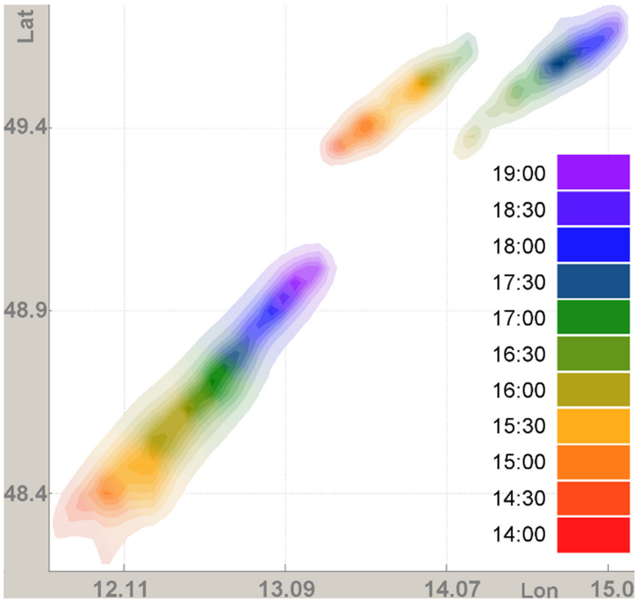

Figure 20. STDmap with smooth color gradient based on curved tendency line and the temporal interval of 30 minutes.

It can be obviously perceived in all STDmaps that the entire density information is clearly visible while the temporal information about phenomena dynamics in terms of speed and moving direction provides the added value. All lightning clusters are moving northeastwards. The upper left cluster is moving faster around 3:30pm than at any other time and it had two density peaks around 3pm and 4pm.

The clear-cut temporal cluster borders reveal another advantage: Density information in layered tints within each specific time interval is clearly visible and separable from neighboring segments. The smooth color transitions between neighboring segments are closer to the reality and correspond better to the visual perception: lightning points occurring for instance some minutes after 3pm can be located inside the 2-3pm segment and points appearing some minutes before 3pm might be placed inside the 3-4pm segment. With the help of an adaptive slider, the smoothing effect can be set for a small time interval (e.g., 14:55 – 15:05) or a large one (maximum smoothing interval: half of the time interval left and right of the temporal border, e.g., 14:30 – 15:30). Moreover, an elastic slider enables the use of different smoothing intervals adaptive to the cluster overlap and thus to the changing cluster speed. In our case we used a threshold of 10 minutes (five minutes before and after each abrupt border line). For an easy comprehension, we suggest to limit the number of colors (time intervals) to no more than about 15. In case of very extensive temporal range, the brightness of the same tone within the same interval can be adopted. For instance, 24 hours can be cut into six by four hours intervals. Within each interval four different brightness of the same tone can be used. In order to verify the proposed color mapping, an extensive user evaluation is necessary.

C. *Wrongly assigned points*

STDmapping approach is suitable for constantly moving SEOs. The approach creates a segmented contour interval for each track. However, the use of abrupt color gradients may lead to temporally wrongly assigned points. The tracking and in particular used clustering method (distance threshold) as well as the temporal segmentation (time intervals and tendency segmentation model) are decisive for the allocation of points to the temporal segments. These decisive steps (parameters) can be adapted to different moving situations along the trajectory. For example, in case a moving SEO changes its speed along the track, temporal intervals and smooth zones could be defined differently in order to reduce wrongly assigned points.

The following two figures illustrate the temporally wrongly assigned points (in black) detected in the STDmap for our test dataset while using a temporal interval of one hour and a linear tendency line. In Figure 21 abrupt temporal borders were used and in Figure 22 smooth zones (for smooth color transitions) of +/- 10 minutes were applied (semi-transparent pink polygons). The number of wrongly assigned points are displayed for each temporal border in Figure 21 and for each temporal interval between the smooth zones in Figure 22. We assume that the smooth zone visually refers to both adjacent temporal intervals. Out of altogether 6885 points for the ‘abrupt’ case 788 points (11.4 %) appeared to be assigned wrong and for the ‘smooth’ case 189 points (2.7 %) appeared to have the wrong temporal color code of the underlying STDmap. Thus, using the smooth STDmap fewer parts are visually allocated to the wrong real temporal interval.

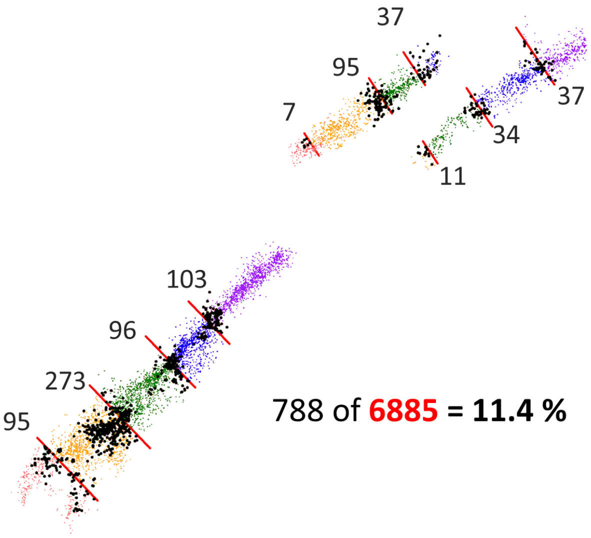

Figure 21. Wrongly assigned points (in black), using abrupt temporal borders.

A lower distance threshold leads to fewer dis-allocated points. The smaller the number of temporal intervals, the more cutlines are defined and probably more temporally false

2015, © Copyright by authors, Published under agreement with IARIA - www.iaria.org

allocated points occur. The wider the smooth area, the fewer the number of wrongly assigned points.

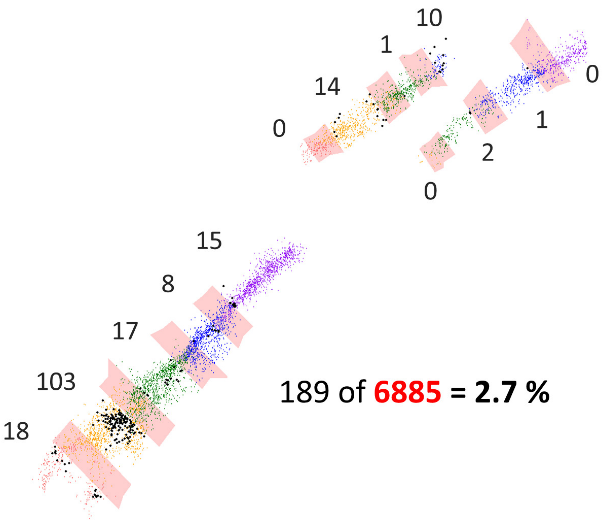

Figure 22. Wrongly assigned points (in black), using smooth temporal borders.

Basically, as the tendency line and segmented cuts are more generalized, the more wrongly assigned points occur. Thus, a spline tendency line should result in less wrongly assigned points than the use of a linear one. If a point is wrongly assigned, then it is mostly behind the segment border to the next temporal interval. A very slow movement consequently results in a higher number of wrongly assigned points. In case a SEO is moving for- and backwards or intersects a lot with itself, the produced contour intervals would overlap and thus map reading becomes more difficult, even if transparency is applied.

Between STDmapping and "KDE maps for each temporal interval" there are certain complementarities. We have shown that both approaches have their pros and cons. Our proposed STDmap is an alternative procedure to the overlapping KDE maps. Surely, there might be applications for which the use of KDE maps is more appropriate and others for which the STDmapping approach is more suitable. For our application case of moving lightning data, we prefer the use of STDmap. Comprehensive user tests are necessary to verify the right choice for different applications.

D. Limitations and comparison with existing approaches

Existing density mapping approaches are able to consider either two moments of time or a series of time intervals within density information visualization in a STC. However, the targeted visual communication of point density changes necessitates user interactions, especially when a cluster of interest is bounded by other clusters, it can be hardly explored without interaction. The 3D density STC suggested by Nakaya and Yano [25] is a comparable approach, where a series of time steps is taken into account within density information visualization with the aim to illustrate the change of point density in time. However, the density changes in time can only be explored interactively by panning, zooming and rotating etc. The STC approach does provide explicit spatio-temporal density information while the STDmapping method assigns some points to the wrong temporal intervals. However, the STC approach needs strong user interaction for the exploration of point density changes. If a cluster of interest is surrounded by other clusters, it can be hardly explored. Our approach has overcome this drawback by storing and presenting temporal information in different colors in a STDmap (in 2D). Spatial and temporal clustering parameters/thresholds can be adapted in order to improve the resulting STDmap. The approach creates appropriate segmented density surfaces. In other words, the approach is suitable if a movement and a main movement direction of the phenomena (polygon) are given and thus a tendency line together with temporal borderlines can be automatically identified. However, several movement cases may cause difficulties to identify the segments: (1) if the SEP is simultaneously expanding in several directions the tendency line needs to be split, which is no trivial task in the practice. (2) If the SEP is moving and returning after a circular track back to a previously passed location/area; or if the SEP is moving for and backwards. In these cases spatio-temporal polygons would overlap significantly and the resulting STDmap may become illegible.

E. Usability of STDmapping

To verify the usability of our approach a comprehensive test of how users interact with the STDmapping is necessary. It deals with a multidisciplinary research field and requires knowledge about the user, the user’s task and the involved technology [42]. The target users of our approach are domain specialists who interact with the visualized dynamic phenomena and who need to identify spatio-temporal changes of local and global point densities. The anticipated user tests aim to investigate how the visualized information is perceived and understood. The usability of alternative STDmaps can be compared or iteratively improved. The iteration bears a two-fold meaning. On the one hand, the STDmap designers benefit from user’s behavior. On the other hand, an improved STDmap will better empower the users. In the latter case, the users get trained to get along with the STDmapping approach. Since the interactive and explorative use of the STDmaps of dynamic SEPs requires some vocational adjustment, the corresponding usability tests should be conceptualized as a long-term endeavor involving repeating test sessions with the same target users.

VI. Conclusion and Future Work

Visualizing density and distribution information is a key support for the understanding of spatio-temporal phenomena represented by point data. However, the temporal information is not yet adequately handled in existing density mapping approaches. Our work has closed this research gap by incorporating and visualizing the temporal change of point cluster in a 2D density map. Our approach is termed as STDmapping according to which a density surface of layered tints can be divided into different temporal segments. Each

2015, © Copyright by authors, Published under agreement with IARIA - www.iaria.org

segment is then visualized by a color hue with varying intensities. The temporal borders are visualized as lines perpendicular to the moving tendency lines. Tendency lines are either straight or curved. Moreover, abrupt or smooth color gradients between neighboring temporal segments can be applied.

The resulted STDmaps comprise spatio-temporal information about density, distribution, movement patterns such as moving direction and speed of dynamic point clusters. Thus, our approach supports the pattern detection/extraction of spatio-temporal phenomena without having to activate interactive tools. Furthermore, our approach can be adapted to dynamic phenomena represented by other point events as well as to moving point groups (e.g., animal swarms).

In the next step of our work, the usability of STDmap for lightning data will be investigated. It requires the participation of users who are domain specialists and should make decisions based on their understanding of visualized lightning data. Specific user tasks related to the extraction of certain spatio-temporal density information or dynamic patterns should be repeatedly conducted and evaluated. Various interactive functions should be made available to allow these users to manipulate the visualization for the purpose of a more efficient exploration, for instance, by adapting the color scheme, changing the time interval, etc.

Meanwhile, we plan to investigate the relation between the characteristics of initial data (density, distribution, spatio-temporal change of point coordinates) and their modeling parameters (movement tendency, time interval, boundary lines) with the purpose to describe the dynamic phenomena with minimum information loss or distortion for the subsequent visualization and use of STDmaps. Furthermore, an adaption of our approach for 3D point data is also possible. Last but not least, it is worthwhile to develop the dynamic mapping technologies for geo-sensory systems, which, for example, demand the dynamic derivation of density layers, contour lines or discrete classes from the values regularly sent by various sensors.

ACKNOWLEDGMENT

The authors gratefully acknowledge Nowcast Company for providing lightning test dataset and the support of the Graduate Center Civil Geo and Environmental Engineering at Technische Universität München, Germany.

REFERENCES

[1] S. Peters and L. Meng, "Spatio Temporal Density Mapping of a Dynamic Phenomenon," in *GEOprocessing 2014 - The Sixth International Conference on Advanced Geographic Information Systems, Applications, and Services*, Barcelona, Spain, 2014, pp. 83-88.

[2] N. Andrienko and G. Andrienko, "Visual analytics of movement: An overview of methods, tools and procedures," *Information Visualization,* vol. 12, pp. 3-24, 2013.

[3] W. A. Mackaness, A. Ruas, and L. T. Sarjakoski, *Generalisation of geographic information: cartographic modelling and applications*. Amsterdam, The Netherlands: Elsevier Science, 2007.

[4] K. Romanenko, D. Xiao, and B. J. Balcom, "Velocity field measurements in sedimentary rock cores by magnetization prepared 3D SPRITE," *Journal of Magnetic Resonance,* pp. 120-128, 2012.

[5] S. Stoilova-McPhie, B. O. Villoutreix, K. Mertens, G. Kemball-Cook, and A. Holzenburg, "3-Dimensional structure of membrane-bound coagulation factor VIII: modeling of the factor VIII heterodimer within a 3-dimensional density map derived by electron crystallography," *Blood,* vol. 99, pp. 1215-1223, 2002.

[6] J. W. Tukey, *Exploratory data analysis*: Addison-Wesley, 1977.

[7] B. W. Silverman, *Density estimation for statistics and data analysis* vol. 26: CRC press, 1986.

[8] N. Cressie, "Statistics for spatial data," *Terra Nova,* vol. 4, pp. 613-617, 1992.

[9] D. W. Scott, *Multivariate density estimation: theory, practice, and visualization* vol. 383: Wiley. com, 2009.

[10] D. O'Sullivan and D. J. Unwin, *Geographic information analysis*: John Wiley & Sons, 2003.

[11] M.-P. Kwan, "Geovisualisation of activity-travel patterns using 3D geographical information systems," in *10th international conference on travel behaviour research (pp. pages pending), Lucerne*, 2003, pp. 185-203.

[12] I. Assent, R. Krieger, E. Müller, and T. Seidl, "VISA: visual subspace clustering analysis," *ACM SIGKDD Explorations Newsletter,* vol. 9, pp. 5-12, 2007.

[13] J. M. Krisp and O. Špatenková, "Kernel density estimations for visual analysis of emergency response data," in *Geographic Information and Cartography for Risk and Crisis Management*, ed: Springer, 2010, pp. 395-408.

[14] R. Maciejewski, S. Rudolph, R. Hafen, A. Abusalah, M. Yakout, M. Ouzzani*, et al.*, "A visual analytics approach to understanding spatiotemporal hotspots," *Visualization and Computer Graphics, IEEE Transactions on,* vol. 16, pp. 205-220, 2010.

[15] C. F. Schmid and E. H. MacCannell, "Basic Problems, Techniques, and Theory of Isopleth Mapping*," *Journal of the American Statistical Association,* vol. 50, pp. 220-239, 1955.

[16] T. A. Slocum, R. B. McMaster, F. C. Kessler, and H. H. Howard, *Thematic cartography and geovisualization*: Pearson Prentice Hall Upper Saddle River, NJ, 2009.

[17] M. Langford and D. J. Unwin, "Generating and mapping population density surfaces within a geographical information system," *The Cartographic Journal,* vol. 31, pp. 21-26, 1994.

[18] E. M. Jansenberger and P. Staufer-Steinnocher, "Dual Kernel density estimation as a method for describing spatio-temporal changes in the upper austrian food retailing market," in *7th AGILE Conference on Geographic Information Science*, 2004, pp. 551-558.

[19] J. M. Krisp and S. Peters, "Directed kernel density estimation (DKDE) for time series visualization," *Annals of GIS,* vol. 17, pp. 155-162, 2011 2011.

[20] J. M. Krisp, S. Peters, and F. Burkert, "Visualizing Crowd Movement Patterns Using a Directed Kernel Density Estimation," in *Earth Observation of Global Changes (EOGC)*, Munich, Germany, 2013, pp. 255-268.

[21] J. M. Krisp, S. Peters, C. E. Murphy, and H. Fan, "Visual Bandwidth Selection for Kernel Density Maps,"

2015, © Copyright by authors, Published under agreement with IARIA - www.iaria.org

Photogrammetrie - Fernerkundung - Geoinformation, vol. 2009, pp. 445-454, 2009/11/01/ 2009.

[22] J. M. Krisp, S. Peters, and M. Mustafa, "Application of an Adaptive and Directed Kernel Density Estimation (AD-KDE) for the Visual Analysis of Traffic Data," in *GeoViz2011*, Hamburg, Germany, 2011.

[23] J. M. Krisp and S. Peters, "Visualizing Dynamic 3D Densities: A Lava-lamp approach," in *13th AGILE International Conference on Geographic Information Science*, Guimaraes, Portugal, 2010, pp. 10-14.

[24] S. Peters and J. M. Krisp, "Density calculation for moving points," in *13th AGILE International Conference on Geographic Information Science*, Guimaraes, Portugal, 2010, pp. 10-14.

[25] T. Nakaya and K. Yano, "Visualising Crime Clusters in a Space time Cube: An Exploratory Data analysis Approach Using Space time Kernel Density Estimation and Scan Statistics," *Transactions in GIS,* vol. 14, pp. 223-239, 2010.

[26] C. F. Schmid and E. H. MacCannell, "Basic Problems, Techniques, and Theory of Isopleth Mapping*," *Journal of the American Statistical Association,* vol. 50, pp. 220-239, 1955.

[27] U. Demšar and K. Virrantaus, "Space–time density of trajectories: exploring spatio-temporal patterns in movement data," *International Journal of Geographical Information Science,* vol. 24, pp. 1527-1542, 2010.

[28] R. Scheepens, N. Willems, H. van de Wetering, G. Andrienko, N. Andrienko, and J. J. van Wijk, "Composite density maps for multivariate trajectories," *Visualization and Computer Graphics, IEEE Transactions on,* vol. 17, pp. 2518-2527, 2011.

[29] N. Willems, H. Van De Wetering, and J. J. Van Wijk, "Visualization of vessel movements," in *Computer Graphics Forum*, 2009, pp. 959-966.

[30] N. Willems, H. Van De Wetering, and J. J. Van Wijk, "Visualization of vessel movements," in *Computer Graphics Forum*, 2009, pp. 959-966.

[31] G. McArdle, A. Tahir, and M. Bertolotto, "Interpreting map usage patterns using geovisual analytics and spatio-temporal clustering," *International Journal of Digital Earth,* pp. 1-24, 2014.

[32] P. Forer and O. Huisman, "Space, time and sequencing: Substitution at the physical/virtual interface," *Information, Place, and Cyberspace: Issues in Accessibility,* pp. 73-90, 2000.

[33] G. Andrienko and N. Andrienko, "A general framework for using aggregation in visual exploration of movement data," *Cartographic Journal,* vol. 47, pp. 22-40, 2002.

[34] H. D. Betz, K. Schmidt, and W. P. Oettinger, "LINET – An International VLF/LF Lightning Detection Network in Europe," in *Lightning: Principles, Instruments and Applications*, H. D. Betz, U. Schumann, and P. Laroche, Eds., ed Dordrecht: Springer Netherlands, 2009, pp. 115-140.

[35] S. Peters, H.-D. Betz, and L. Meng, "Visual Analysis of Lightning Data Using Space–Time-Cube," in *Cartography from Pole to Pole - 26th International Cartographic Conference (ICC)*, Dresden, Germany, 2013, pp. 165-176.

[36] S. Peters and L. Meng, "Visual Analysis for Nowcasting of Multidimensional Lightning Data," *ISPRS International Journal of Geo-Information,* vol. 2, pp. 817-836, 2013.

[37] S. Peters, L. Meng, and H. D. Betz, "Analytics approach for Lightning data analysis and cell nowcasting," in *EGU General Assembly Conference Abstracts*, 2013, pp. 32-3.

[38] C. De Boor, *A practical guide to splines* vol. 27: Springer-Verlag New York, 1978.

[39] D. Borland and R. M. Taylor II, "Rainbow color map (still) considered harmful," *IEEE Computer Graphics and Applications,* vol. 27, pp. 14-17, 2007.

[40] C. Brewer and M. Harrower. (2014, 10/2014). *colorbrewer*. Available: http://www.colorbrewer2.org/

[41] R. Wicklin. (2013, 10/2014). *How to choose colors for maps and heat maps*. Available: http://blogs.sas.com/content/iml/2014/10/01/colors-for-heat-maps/

[42] M. Haklay, *Interacting with geospatial technologies*: Wiley Online Library, 2010.

2015, © Copyright by authors, Published under agreement with IARIA - www.iaria.org